Gene deregulation and spatial genome reorganization near breakpoints prior to formation of translocations in anaplastic large cell lymphoma

Stephan Mathas[a,b,1], Stephan Kreher[a,b], Karen J. Meaburn[c], Korinna Jöhrens[d], Björn Lamprecht[a,b], Chalid Assaf[e], Wolfram Sterry[e], Marshall E. Kadin[f,g], Masanori Daibata[h], Stefan Joos[i], Michael Hummel[d], Harald Stein[d], Martin Janz[a,b], Ioannis Anagnostopoulos[d], Evelin Schrock[j], Tom Misteli[c], and Bernd Dörken[a,b]

[a]Max-Delbrück-Center for Molecular Medicine, Robert-Rössle-Strasse 10, 13125 Berlin, Germany; [b]Hematology, Oncology, and Tumorimmunology, Charité, Medical University Berlin, Campus Virchow Klinikum, Augustenburger Platz 1, 13353 Berlin, Germany; [c]Cell Biology of Genomes, National Cancer Institute, National Institutes of Health, 41 Library Drive, Bethesda, MD 20892; [d]Institute of Pathology, Charité, Medical University Berlin, Campus Benjamin Franklin, Hindenburgdamm 30, 12200 Berlin, Germany; [e]Department of Dermatology, Allergy, and Venerology, Skin Cancer Center Charité, Medical University Berlin, Charitéplatz 1, 10117 Berlin, Germany; [f]Department of Pathology, Harvard Medical School, Boston, MA 02115; [g]Department of Dermatology, Boston University, and Roger Williams Medical Center, 50 Maude Street, Providence, RI 02908; [h]Department of Hematology, Kochi Medical School, Kohasu, Okoh-cho, Nankuko-city, Kochi 783-8505, Japan; [i]German Cancer Research Center, B060, Im Neuenheimer Feld 280, 69120 Heidelberg, Germany; and [j]Institute for Clinical Genetics, Dresden University of Technology, Fetscherstrasse 74, 01307 Dresden, Germany

Communicated by Mark T. Groudine, Fred Hutchinson Cancer Research Center, Seattle, WA, January 30, 2009 (received for review October 23, 2008)

Although the identification and characterization of translocations have rapidly increased, little is known about the mechanisms of how translocations occur in vivo. We used anaplastic large cell lymphoma (ALCL) with and without the characteristic t(2;5)(p23;q35) translocation to study the mechanisms of formation of translocations and of ALCL transformation. We report deregulation of several genes located near the ALCL translocation breakpoint, regardless of whether the tumor contains the t(2;5). The affected genes include the oncogenic transcription factor Fra2 (located on 2p23), the HLH protein Id2 (2p25), and the oncogenic tyrosine kinase CSF1-receptor (5q33.1). Their up-regulation promotes cell survival and repression of T cell-specific gene expression programs that are characteristic for ALCL. The deregulated genes are in spatial proximity within the nuclear space of t(2;5)-negative ALCL cells, facilitating their translocation on induction of double-strand breaks. These data suggest that deregulation of breakpoint-proximal genes occurs before the formation of translocations, and that aberrant transcriptional activity of genomic regions is linked to their propensity to undergo chromosomal translocations. Also, our data demonstrate that deregulation of breakpoint-proximal genes has a key role in ALCL.

cancer genetics | signal transduction | nuclear architecture | lymphomatoid papulosis

Balanced chromosomal translocations are a hallmark of cancer cells, and are thought to be important, if not causal, for hematopoietic and mesenchymal tumorigenesis (1). At the molecular level, translocations generally result in either altered expression of genes located directly at a breakpoint, or in fusion of genes located at the 2 breakpoints (1). In most cases, the affected genes are transcription factors or tyrosine kinases, and the translocation generally leads to their inactivation or constitutive activation. This defect often causes inhibition of differentiation or uncontrolled proliferation. Nevertheless, translocations are, at least in some cases, not sufficient to fully transform cells, because chromosomal disease-associated translocations are present in healthy individuals (2), and transgenic mice expressing known tumor fusion proteins do not spontaneously develop tumors in most cases (1, 2).

The translocation t(2;5)(p23;q35) is characteristic for anaplastic large cell lymphoma (ALCL), a subgroup of peripheral T cell lymphomas (TCL) (3, 4). By fusion of the 5′ oligomerization domain of the nucleophosmin (*NPM1*) gene (located on 5q35) with the 3′ anaplastic lymphoma kinase (*ALK*) tyrosine kinase domain (2p23), this translocation results in a NPM-ALK fusion protein with constitutive activation of the ALK kinase (3). Several questions regarding the pathogenesis of ALCL are unresolved. First, in ≈40% of systemic ALCL, the translocation t(2;5) is not present (4), suggesting yet unknown alternative mechanisms of transformation. Second, the expression of NPM-ALK per se might not be sufficient for malignant transformation to ALCL, because NPM-ALK expression leads to non-ALCL malignancies in animal models (3). Third, morphological similarities and molecular defects are found in both ALCL types, independent of the translocation t(2;5) (4–6). Last, systemic ALCL may arise from primary cutaneous $CD30^+$ lymphoproliferative disorders such as lymphomatoid papulosis (LyP) in up to 20% of cases (7). The mechanism of this progression is not understood.

Although the identification and characterization of translocations have rapidly increased, little is known about how translocations occur in vivo (1, 8). Obviously, double-strand breaks (DSBs) of involved chromosomes have to occur, and broken ends have to meet each other in the nucleus. Two hypotheses have been proposed to explain how translocations arise: the "contact-first" model postulates that chromosome fibers have to colocalize at the time of DNA damage (9), whereas the "breakage-first" model states that broken chromosome ends can move in the nuclear space to find their translocation partner (10). Although formal evidence is currently lacking, recent data favor the contact-first model as the underlying mechanism required for formation of translocations in mammalian cells (8, 9, 11–13).

Here, we set out to study the mechanism of translocation formation and of ALCL transformation by the analysis of ALCL either carrying or lacking the characteristic t(2;5). We describe a number of deregulated genes surrounding the breakpoint regions on chromosomes 5 and 2 in both ALCL cells with and without the characteristic translocation. Also, we show that the breakpoint regions in t(2;5)-negative ALCL cells are in spatial proximity within the nuclear space, and that this proximity predisposes for induction of t(2;5).

Results

Deregulation of Breakpoint-Proximal Genes Regardless of t(2;5). We first probed the expression levels of genes near the ALCL breakpoint on chromosomes 5 and 2, and in the surrounding regions. We focused on genes with known or assumed oncogenic functions and a

Author contributions: S.M., K.J.M., C.A., S.J., T.M., E.S., and B.D. designed research; S.M., S.K., K.J.M., K.J., B.L., M.H., H.S., and I.A. performed research; M.E.K. and M.D. contributed new reagents/analytic tools; S.M., S.K., K.J.M., K.J., B.L., C.A., W.S., S.J., M.H., H.S., M.J., I.A., E.S., T.M., and B.D. analyzed data; and S.M., K.J.M., M.J., T.M., and B.D. wrote the paper.

The authors declare no conflict of interest.

[1]To whom correspondence should be addressed. E-mail: stephan.mathas@charite.de.

This article contains supporting information online at www.pnas.org/cgi/content/full/0900912106/DCSupplemental.

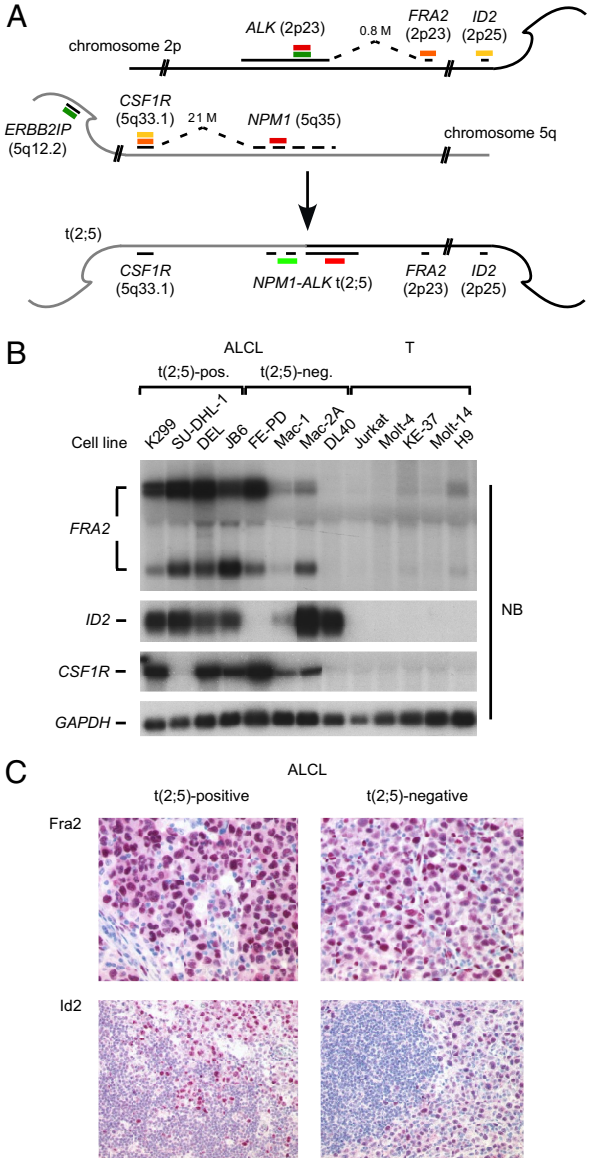

Fig. 1. Up-regulation of breakpoint proximal genes in ALCL regardless of t(2;5). (*A*) Localization of the analyzed genes *FRA2* (located on 2p23), *ID2* (2p25), and *CSF1R* (5q33.1). In the case of t(2;5), the fusion of *NPM* (5q35) and *ALK* (2p23) results in the *NPM-ALK* fusion gene. Colored bars indicate positions of probes used for FISH in Fig. 4 *A* and *C*. (*B*) Analysis of *FRA2*, *ID2*, and *CSF1R* mRNA expression in various cell lines by Northern blot analysis (NB). Expression of *GAPDH* was analyzed as a control. (*C*) Immunohistochemistry of Fra2 and Id2 in ALCL carrying (*Left*) or lacking (*Right*) t(2;5). Cells with positive signals are stained in red. Large neoplastic cells show a strong nuclear staining for Fra2 and Id2, whereas no (Fra2) or only weak (Id2) signals are detectable in the small nonneoplastic cells. (Original magnification, 80×.)

presumed role in ALCL pathogenesis: the helix–loop–helix (HLH) factor inhibitor of differentiation 2 (*ID2*; located on 2p25), which inhibits cellular differentiation, promotes cellular growth, and mediates reprogramming of Hodgkin lymphoma cells (14, 15), the oncogenic AP-1 transcription factor *FRA2* (2p23; also called FOS-like antigen 2, *FOSL2*) (16), and the oncogenic tyrosine kinase CSF-1 receptor (*CSF1R*; 5q33.1) (17, 18) (Fig. 1*A*). The analysis of a panel of T cell-derived ALCL cell lines, including 4 cell lines carrying t(2;5) and 4 lacking t(2;5) revealed aberrantly high levels of Fra2, Id2 and CSF1R mRNA and protein expression (Fig. 1*B* and Fig. S1*A*). Remarkably, we found up-regulation of these genes even in the absence of t(2;5). In contrast, all non-ALCL T cell-derived control cell lines lacked expression of these genes. The analysis of the various cell lines for expression of NPM, ALK, and NPM-ALK by Western blot and RT-PCR analyses showed the expected results, i.e., expression of NPM-ALK is restricted to t(2;5)-positive ALCL cell lines (Fig. S1*B*).

Elevated levels of these proteins were confirmed in tissue sections from t(2;5)-positive and t(2;5)-negative ALCL patient samples (Fig. 1*C* and Table S1). We detected high expression of Fra2 and, in accordance with previously published data (19), of Id2 in all 10 t(2;5)-positive ALCL cases, and in 9/15 (Fra2) and 15/15 (Id2) t(2;5)-negative ALCL tumor samples. In contrast, Fra2 was not detected, and Id2 was expressed at a much lower level in only a subset of lymphoid cells in normal lymphoid tissue, including nonmalignant lymphoid cells present in all ALCL samples and in samples from activated human palatine tonsil, thymus, and spleen (Fig. S1*C* and Table S1). Also, expression of Fra2 was neither detectable in the tumor cells of 8 peripheral TCL cases containing large numbers of atypical $CD30^+$ cells nor in 46 cases of diffuse large B cell lymphoma of the most common morphologic variants. The T lineage-inappropriate expression of the macrophage-specific CSF1R in ALCL cells even exceeded the expression level found on CD33-positive cells isolated from healthy donors. Given the unusual high and aberrant expression of these genes in ALCL, we assayed for alterations in copy number for *FRA2* and *ID2* by FISH (Fig. S1*D*). We found additional copy numbers of *FRA2* in 75% (6/8) of t(2;5)-positive, and 50% (4/8) of t(2;5)-negative ALCL patient cases; and of *ID2* in 71.4% (5/7) of t(2;5)-positive, and 50% (3/6) of t(2;5)-negative cases, respectively. Together, these observations suggest that breakpoint-proximal genes have a fundamental role in ALCL biology in a translocation-independent fashion.

Characterization and Consequences of the Constitutively Activated AP-1 Complex. To determine the functional consequences of elevated Fra2 expression in ALCL, we first analyzed AP-1 DNA binding activity, which revealed a unique activity restricted to all of the ALCL cell lines (Fig. 2*A*). Electrophoretic mobility shift assay performed with a broad panel of antibodies recognizing Jun (c-Jun, JunB, and JunD), Fos (c-Fos, Fra1, and Fra2), or ATF (ATF-2 and ATF-3) members revealed a striking similarity of the AP-1-complex in all ALCL cells with reactivity for JunB and Fra2, regardless of t(2;5) (Fig. S1*E*). The main interaction partner of Fra2 was the AP-1 family member JunB, as shown by co-immunoprecipitation (Fig. 2*B*; the IP with the isotype control antibody did not show any specific coIP). The *JUNB* gene locus is amplified and JunB is overexpressed in ALCL, and the AP-1 activity protects these cells from apoptosis (20, 21). Our data suggest that these functions are at least in part mediated by its interaction partner Fra2. To further investigate whether Fra2-JunB complexes protect lymphoid cells from apoptosis, we investigated their function after forced expression in IL-3 dependent Ba/F3 cells, which serve as a model for growth factor independence induced by the gene of interest. We generated stably transfected Ba/F3 cell clones with empty plasmid (Mock), or expressing Fra2 (FLAG-tagged; Fra2) or a Fra2-JunB single-chain construct (Fra2-JunB; Fra2 and JunB joined by a flexible polypeptide tether) (Fig. 2*C* and Fig. S1*F*). We measured the response of several Mock-transfected clones (clones 1, 2, and 3), 3 Fra2-expressing (clones 5, 13, and 35), and 2 Fra2-JunB-expressing clones (clones 30 and 61) to IL-3 withdrawal. As expected, Mock clones survived IL-3 withdrawal for no longer than 6–7 days. In contrast, all Fra2 or Fra2-JunB clones survived IL-3 withdrawal for >10 days (Fig. 2*C*). Together, these data demonstrate a recurrent alteration of Fra2 in a human malignancy and argue for the Fra2-JunB AP-1 complex as an important factor for transformation of t(2;5)-positive and t(2;5)-negative ALCL cells.

The Id2-Mediated Loss of T Cell Phenotype in ALCL. Next, we examined the consequences of the aberrant Id2 expression in ALCL. Id

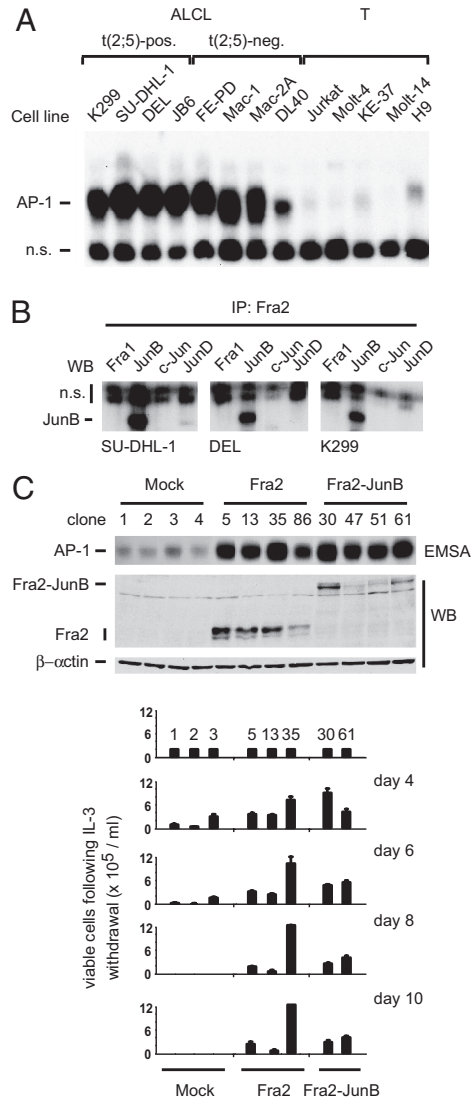

Fig. 2. Characterization of the constitutively active AP-1 complex in ALCL cells. (*A*) EMSA of transcription factor AP-1 in nuclear extracts of various cell lines. n.s., nonspecific band, not the free probe. (*B*) CoIP of Fra2 and JunB. IP of Fra2 was performed in whole-cell extracts. Coprecipitated proteins were detected by Western blot analysis using antibodies specific for Fra1, JunB, c-Jun, and JunD. (*C*) Fra2 or Fra2-JunB protect Ba/F3 cells from IL-3 withdrawal. Representative stably transfected cell clones expressing FLAG-tagged Fra2 (clones 5, 13, 35, and 86) or a Fra2-JunB single-chain construct (clones 30, 47, 51, and 61), and respective Mock clones (clones 1, 2, 3, and 4) were analyzed by EMSA for AP-1 DNA binding activity (*Upper*), and for Fra2 and Fra2-JunB protein expression by Western Blot analysis using a Fra2-specific antibody; β-actin was analyzed as a control. (*Lower*) Representative Ba/F3 clones with different Fra2 or Fra2-JunB expression levels were starved from IL-3. Viable cells were counted at the days indicated. Error bars indicate SDs.

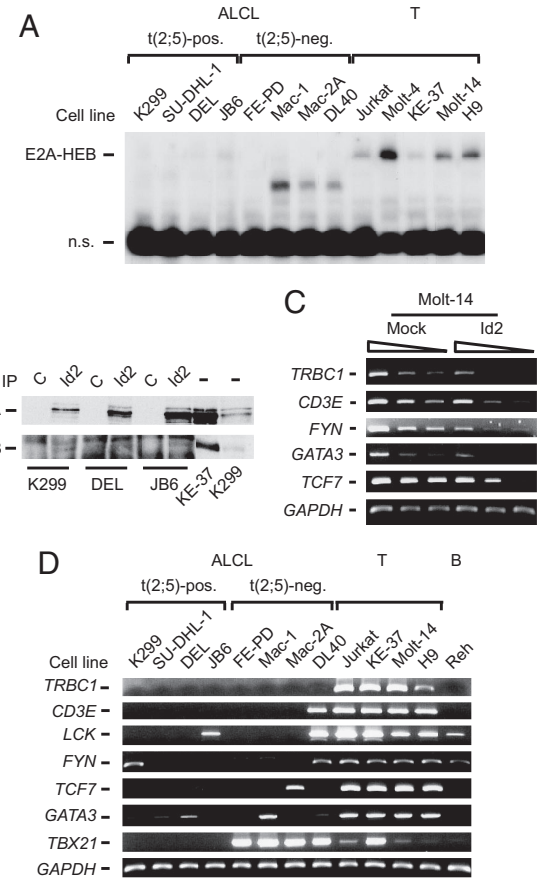

Fig. 3. The Id2-mediated loss of T cell phenotype in ALCL. (*A*) Nuclear extracts of the various cell lines were analyzed by EMSA for E-box DNA binding activity. Positions of specific complexes (E2A-HEB) are indicated. n.s., nonspecific band, not the free probe. (*B*) CoIP of Id2-E2A and Id2-HEB complexes. Lysates of K299, DEL, and JB6 cells were immunoprecipitated with antibody to Id2 or the respective control (C). Coprecipitated E2A and HEB proteins were detected by WB. Far right (−), whole-cell extracts of KE-37 and K299 cells. (*C*) RT-PCR analysis of Molt-14 cells transfected with vector only (Mock) or Id2 expression plasmid along with pEGFP-N3. Input cDNA was diluted 1:1, 1:5, and 1:10 as indicated by triangles. T cell-associated genes were assessed by RT-PCR in enriched GFP$^+$ cells. *GAPDH* was analyzed as a control. (*D*) Messenger RNA expression of T cell-associated genes by RT-PCR in various cell lines. T cell-derived cell lines (T) served as positive, B cell-derived Reh cells as a negative control. Genes *LCK* and *FYN* are expressed in B and T cells. *GAPDH* was analyzed as a control.

proteins contain a HLH dimerization motif, but lack the basic region required for DNA binding (15). The interaction of Id proteins with basic (b)HLH proteins, including E2A and HEB, prevents binding to DNA and, thus, inhibits transcription (14, 15). Because E2A and HEB are known to regulate expression of many T cell-associated genes (22), we investigated their expression and DNA binding activity (Fig. 3*A* and Fig. S2*A*). Although HEB (encoded by the gene *TCF12*) and E2A (encoded by the gene *TCF3*) were expressed in ALCL cells (Fig. S2*A*), they lacked E-box DNA-binding activity almost completely (Fig. 3*A*), again regardless of the presence of t(2;5). In contrast, in all non-ALCL T cell-derived cells E-proteins bound to DNA, which mainly consisted of E2A-HEB heterodimers (Fig. 3*A* and Fig. S2*B*). These data indicated a functional inhibition of bHLH proteins in ALCL. To detect an interaction of the bHLH proteins E2A or HEB with Id2, which might mediate such an inhibition, we performed coIPs (Fig. 3*B*). Id2 interacted with E2A, and coIP was also observed with HEB. These results suggest that E-box DNA-binding in ALCL is primarily inhibited by an interaction with the aberrantly expressed Id2 protein. To directly address the consequences of Id2 overexpression for the expression of T cell-associated genes, we transfected T cell-derived Molt-14 cells with Id2 (Fig. 3*C* and Fig. S2*C*). Consistent with our prediction, we observed an Id2-mediated decrease of expression of several T cell-associated genes [*CD3E*, *TRBC1* (encoding T cell receptor beta constant region 1), *FYN*, *TCF7* (encoding TCF-1), and *GATA3*) (Fig. 3*C*). In line with these data, ALCL cells not only show a loss of TCR expression (23), but also of TCR-associated signaling molecules (*LCK* and *FYN*) and T cell-associated transcription factors [TCF1 (encoded by the gene *TCF7*, T-bet (encoded by the gene *TBX21*), and GATA3] (Fig. 3*D*, Fig. S2*D*, and Table S1). Together, these data suggest that aberrant

Id2 expression mediates the loss of T cell differentiation in ALCL regardless of t(2;5).

Spatial Proximity of 5q and 2p in t(2;5)-Negative ALCL. Our analyses indicated that deregulation of the above described genes was restricted to ALCL and was independent of t(2;5). We hypothesized that the aberrant activation of these genes in t(2;5)-negative cells might be related to the formation of t(2;5). In particular, we speculated that chromatin structure is altered at these sites before the formation of translocations, and that these changes lead to aberrant expression of genes in the flanking regions and possibly predispose these sites to translocations. To test this hypothesis, we measured the proximity of the various gene loci on chromosomes 5 and 2 using 2-color FISH (Fig. 4*A*, positions of the probes are shown in Fig. 1*A*). Gene copy numbers of the various gene loci for all t(2;5)-negative ALCL and control cell lines investigated are shown in Table S2. The t(2;5)-positive ALCL cell lines K299 and JB6 served as positive controls. As expected because of the reciprocal t(2;5), *NPM1-ALK* (5q35–2p23), *CSF1R-FRA2* (5q33.1–2p23), and *CSF1R-ID2* (5q33.1–2p25) were in close spatial proximity (defined as <400 nm apart) in 78–100% of the K299 or JB6 nuclei (Fig. 4*A*). In contrast, we detected little spatial proximity for these gene pairs in the non-ALCL cell lines Jurkat and KE-37 (<10% of the nuclei showed proximity), in which these genes are not expressed. Intriguingly, in all ALCL cell lines lacking t(2;5), these gene pairs were in spatial proximity in a significant fraction of cells (10.6–22.5%; DL-40 cells were not included in this analysis due to the increased copy numbers of all of the various genes to 4–6 copies in this cell line). These values are in line with proximity frequencies observed between other translocation partners and nonrandomly paired genes (12, 24). As a further control, *NPM1* (5q35) and *ALK* (2p23) were not found in proximity to *ZO-1* (15q13), which is not a translocation partner. All genes were present in 2 copies, except *ALK*, *FRA2*, and *ID2*, which were triploid in a significant proportion of Mac-2A and FE-PD cells (Table S2). However, the extra allele does not bias the colocalization results in these cell lines, because *ALK* (3 copies) colocalizes with the control gene ZO-1 (2 copies) in a highly similar fraction of the nuclei as compared with the control cell lines Jurkat and KE-37, and the frequency of colocalization between *CSF1R* and *FRA2* are the same in t(2;5)-negative ALCL cell lines, which contain either 2 or 3 *FRA2* alleles. Also, the frequency of colocalization detected for *ZO-1* to either *NPM1* or *ALK* does not significantly differ from each other in both Mac-2A and FE-PD. In all ALCL lines analyzed, but not in the control T cell-derived lines KE-37 or Jurkat, *ERBB2IP* (5q12.2) and *ALK* were also seen in spatial proximity (Fig. 4*A*), indicating that spatial proximity of 5q and 2p applied to larger genome regions. We also observed increased proximity of *CSF1R-FRA2*, and *CSF1R-ID2* in H9 cells, which might be due to the increased copy numbers to 3–4 copies of these genes in this cell line (Table S2), as highlighted by the fact that the control *ZO-1-NPM1* pair also shows elevated proximity, and due to the elevated level of Fra2 (Fig. 1*B*). Additional translocations involving chromosomes 2 and 5 in t(2;5)(p23;q35)-negative cell lines, which might influence the results of the proximity analyses, were excluded by spectral karyotyping (SKY).

Induction of t(2;5) in Cell Lines with Spatial Proximity of 5q and 2p. Having demonstrated spatial proximity of the putative translocation partners in t(2;5)-negative ALCL cells, we hypothesized that their proximity facilitates formation of t(2;5). To directly test this hypothesis, we induced DSBs in t(2;5)-negative ALCL and non-ALCL cell lines by ionizing radiation (IR), and performed 2-color FISH for *NPM1* and *ALK* to detect translocations t(2;5), and used LSI *ALK* to visualize DNA breaks within the *ALK* locus (Fig. 4 *B* and *C*). In control experiments, we established conditions for cell survival, and verified DSB and repair efficiency (Fig. S2*E*). In the control cell lines Jurkat and KE-37, in which 5q and 2p are not in spatial proximity, no induction of t(2;5) was observed (Fig. 4*B*). In contrast, translocations t(2;5) were present in metaphases of irradiated Mac-2A and H9 cells (Fig. 4 *B* and *C*), in both of which regions of 5q and 2p are in spatial proximity (Fig. 4*A*).

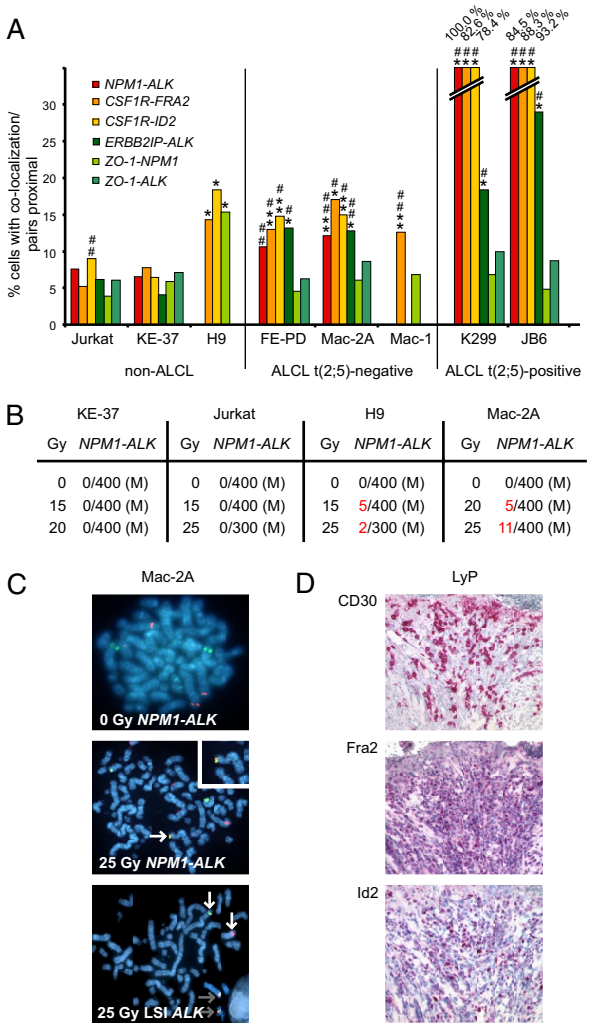

Fig. 4. Analysis of spatial proximity of 5q and 2p. Induction of the translocation t(2;5) in cells with spatial proximity of 5q and 2p. (*A*) Two color FISH of the spatial proximity of indicated gene pairs was performed in various cell lines. The percentage of cells with at least 1 pair of heterologous loci in close spatial proximity (defined as <400 nm apart) is shown. *, statistical significance (ss) at $P < 0.05$ to both Jurkat and KE-37 control cell lines; **, ss at $P < 0.05$ to one of these cell lines; #, ss at $P < 0.05$ to both *ZO-1-ALK/NPM1* control pairs; ##, ss at $P < 0.05$ to 1 *ZO-1* control pair. (*B*) Induction of t(2;5) in cells with spatial proximity of 5q and 2p; 24 h after IR, metaphases were analyzed by 2-color FISH for *NPM1* and *ALK*. Cells with t(2;5) were scored per 400 metaphases, where possible. (*C*) FISH analyses for *NPM1* (green), *ALK* (red), or LSI *ALK* (green-red) as indicated. Representative metaphase spreads of Mac-2A cells are shown. Two signals for *NPM1* and 3 for *ALK* were detectable in untreated cells (*Top*). One metaphase spread of irradiated cells hybridized with *NPM1* and *ALK* with translocation t(2;5) is exemplified (*Middle*). Inset, chromosome with *NPM1-ALK* fusion signal. (*Bottom*) Metaphase spread of irradiated cells hybridized with the LSI *ALK* dual color, break-apart rearrangement probe, which proves breakage of the *ALK* locus. Gray arrows, 2 native *ALK* loci showing fused orange/green signals. White arrows, split red and green signal indicating breakage of the *ALK* locus. (*D*) IHC of a LyP case for CD30, Id2, and Fra2. IHC for CD30 (*Top*; included as a marker for LyP cells), Fra2 (*Middle*), and Id2 (*Bottom*) of 1 representative LyP case is shown (cells with positive signals stain red). Original magnification, 70×.

Aberrant Expression of Fra2 and Id2 in LyP. Given the fact that $CD30^+$ cutaneous lymphoproliferative disorders (CD30-CLD), in particu-

lar LyP, might progress to systemic ALCL (7), we predicted that overexpression of genes identified in our work should be found in a proportion of patients suffering from LyP. We analyzed 11 cases of LyP by immunohistochemistry for the expression of Fra2 and Id2 (Fig. 4*D* and Table S1). In contrast to normal lymphoid cells (Fig. S1*C*), in all LyP cases aberrant expression of Fra2 and Id2 was detectable in the large atypical CD30$^+$ cells. Generally, in contrast to systemic ALCL the expression level in LyP was lower, and the percentage of positive cells for both proteins varied among the cases (Table S1).

Discussion

Here, we have identified several novel hallmarks of ALCL and spatial reorganization of the 2 chromosomes involved in the ALCL-characteristic translocation t(2;5)(p23;q35). Remarkably, we found that deregulation of several genes located in the putative breakpoint regions and spatial reorganization are independent of t(2;5). These data suggest that the formation of t(2;5) might not be the first step leading to malignant transformation, and might not be required for formation of systemic ALCL. This model fits well with the facts that (*i*) in a significant fraction of ALCL cases, t(2;5) is not found (4), (*ii*) although being transforming, the NPM-ALK fusion protein is not sufficient to induce ALCL-like tumors in animal models (4, 25), and (*iii*) a significant number of patients with t(2;5)-positive, CD30$^+$ lymphoproliferations restricted to the skin without systemic dissemination has been reported (26, 27). We focused in our work on the most common *ALK* rearrangement t(2;5)/*NPM1-ALK*, therefore the impact of chromosomal spatial reorganization on the formation of the rare other *ALK*-involving rearrangements (3) remains to be investigated.

The observed deregulation of several t(2;5) breakpoint-proximal genes in ALCL provides insight into the disease mechanism. First, we describe a unique overexpression of the AP-1 complex in nearly all ALCL cases. AP-1 proteins have transforming capacity (16), and they have been implicated in the pathogenesis of various hematopoietic malignancies (20, 28, 29). The up-regulation of JunB in ALCL reported previously (20, 21) and confirmed in this study, and in particular the deregulated Fra2 expression with an intriguing specificity for ALCL, strongly argues for the AP-1 complex as a key factor for transformation of t(2;5)-positive and t(2;5)-negative ALCL cells. Second, we identified an Id2-mediated disruption of the T cell-specific gene expression program in ALCL. Also, the Id2-mediated loss of E2A activity might be linked to tumor progression, because E2A acts as a tumor suppressor in the lymphoid compartment (30, 31). Third, the tyrosine kinase receptor for CSF1 (CSF1R) is expressed in ALCL cells at an unusual high level. At such a high expression level, CSF1R autophosphorylation might support malignant transformation and dedifferentiation (17, 18, 32). Together, these data strongly suggest that the up-regulation of breakpoint-proximal genes is a key event in ALCL biology, independent of the translocation t(2;5). This interpretation does clearly not preclude that, if it arose, the translocation product NPM-ALK provides a growth advantage for t(2;5)-positive ALCL cells. Thus, such a growth advantage, together with the very limited number of patient cases with serial biopsies during disease development, might have so far prevented the identification of a ALCL patient showing transformation from an t(2;5)-negative to an t(2;5)-positive ALCL. The favorable clinical outcome of t(2;5)-positive compared with t(2;5)-negative ALCL (4) might be due to the immunogenicity of ALK, or susceptibility to, for example, chemotherapy-induced DNA damage due to the strong activation of an oncogene, NPM-ALK (33, 34). Our interpretation does not argue against the (provisional) recognition of 2 distinct ALCL entities in the new WHO classification of lymphoid tumors, because this separation is mainly based on the presence or absence of *ALK* rearrangements (35).

CD30-CLD and in particular LyP may be associated with systemic ALCL (7). We revealed in LyP cases an aberrant expression of Fra2 and, in agreement with recent observations (19), Id2. These data support the view of a pathogenetic link between these disease entities. The fact that the level of aberrantly expressed Fra2, but also Id2, in LyP was lower compared with systemic ALCL implies that gene dosage might be involved in progression and invasiveness of these diseases.

The analysis of the spatial location of the putative breakpoint regions in interphase nuclei revealed that they are frequently in close spatial proximity in t(2;5)-negative ALCL cells. This finding is in line with the recent realization that interphase chromosomes are nonrandomly positioned in the cell nucleus (36, 37). Also, recent data demonstrated that, in mammalian cells, broken chromosome ends are immobilized after DNA breakage (11). These data support the contact-first model, which proposes that translocations preferentially occur between neighboring chromosomes (9). Indeed, translocation partners are preferentially in spatial proximity before undergoing rearrangements, which has been shown for frequent partners of translocations in human lymphomas and leukemias (8, 12, 13). We have extended these observations here by demonstrating that t(2;5) is induced in 2 cell lines in which 5q and 2p are in spatial proximity, but not in cell lines in which these 2 chromosomes are distal from each other. These data strongly support a role for spatial proximity in the formation of chromosomal translocations.

The fact that deregulation of genes proximal to the breakpoint is accompanied by spatial juxtaposition of the 2 regions suggests a functional link. An intriguing possibility is that inappropriate activity of ALCL-specific genes near the breakpoints leads to their physical association in 3D space due to their association with shared transcription sites within the cell nucleus. A paradigm for such transcription-mediated clustering of active genes comes from yeast, where tRNA genes cluster near the nucleolus, and actively transcribed tRNA genes exhibit higher recombination frequencies compared with inactive ones (38). In mammalian cells, transcription leads to physical association of the known translocation partners *myc* and *IgH* with each other (24, 37). This interpretation is in line with the fact that transcription factor AP-1 is involved in the regulation of several genes that are deregulated in ALCL, namely Fra2 and JunB itself, Id2, and CSF1R (18, 20, 39). These observations open the possibility that, due to their aberrant activation, these gene loci might be corecruited to a shared transcription factory, thereby increasing the potential for a chromosomal translocation.

Together, our data provide insights into the development and progression of ALCL and demonstrate a link between transcriptional activity of genome regions and their propensity to undergo chromosomal translocations.

Materials and Methods

Cell Lines and Culture Conditions. ALCL (K299, SU-DHL-1, DEL, JB6, all t(2;5)-positive; Mac-1, Mac-2A, FE-PD, DL40, all t(2;5)-negative) and T cell leukemia derived (Jurkat, Molt-4, KE-37, Molt-14, H9) cell lines were cultured as described (20). Electroporation of Molt-14 cells with 40 μg of a pcDNA3-FLAG-Id2 expression plasmid (14) or the respective pcDNA3 control plasmid (Mock; Invitrogen) was performed in OPTI-MEM I by using a Gene-Pulser II (Bio-Rad) with 960 μF and 0.26 kV. Transfection efficiency was determined by pEGFP-N3 (10 μg; Clontech Laboratories) cotransfection and subsequent FACS analysis. Enrichment of transfected cells was performed by FACS sorting of GFP positive cells 48–72 h after transfection by using FACS Vantage and CELLQuest software (Becton Dickinson). Ba/F3 cells were cultured in full medium (20) containing 1.5 ng/mL mIL-3 (PeproTech). Stably transfected Ba/F3 cell clones were generated by electroporation of cells (960 μF, 0.18 kV) with 30 μg of a FLAG-Fra2 construct, a Fra2-JunB single-chain construct (40), or pcDNA3 empty plasmid (Mock; Invitrogen) followed by selection of cell clones with 1.2 mg/mL G418 (Gibco, Invitrogen). For IL-3 withdrawal experiments, cells were counted at the indicated times in a Neubauer chamber after Trypan-blue staining.

RNA Preparation, Northern Blot Analysis, and RT-PCR. Total RNA preparation and Northern blot analysis were described previously (20). Membranes were hybridized with [α-^{32}P]dCTP-labeled random prime-labeled DNA probes. Furthermore, first strand cDNA-synthesis was performed by use of the first strand cDNA syn-

thesis Kit (AMV; Roche), and mRNA expression was analyzed by RT-PCR (*SI Appendix*).

EMSA and Western Blot Analysis. Whole-cell and nuclear extract preparation, EMSA, and Western blot analysis were performed as described (14, 20). Antibodies used for supershift and Western blot analyses are indicated in *SI Appendix*.

CoIP Assays. CoIP of Id2 and E2A or HEB was performed as described (14). Antibodies used for Western blot analysis were E2A (E47/E12; clone G98-271) and HEB (sc-357). For Fra2 coIP, 1×10^7 cells were lysed in buffer containing 20 mM Hepes, pH 7.9/350 mM NaCl/1 mM $MgCl_2$/0.5 mM EDTA/0.1 mM EGTA/1% Nonidet P-40/0.5 mM DTT and a protease inhibitor mixture (Roche). The supernatant containing whole cell extracts was diluted 1:2.5 with buffer containing 20 mM Tris·HCl, pH 7.5/1 mM EDTA. CoIP was performed by using 1,000 μg of protein extract with 2 μg of the Fra2 antibody (Q-20) or the respective isotype control. Western blot analyses of Fra2 IPs were performed by use of the MiniProtean II Multiscreen Apparatus (Bio-Rad).

FISH and Quantitative Measurements. For 3D interphase (i)FISH, growing cell suspensions were incubated on poly-L-lysine-coated coverslips (BD Biosciences) for 1 h at 37 °C. Coverslips were rinsed in 0.3 × PBS for 40–60 s, fixed for 10 min in 4% paraformaldehyde/0.3 × PBS, and washed 3 times in 1 × PBS. Subsequent (i)FISH steps were performed as previously described for 2D cultured cells (41) using various BACs (*SI Appendix*). After performing dual color (i)FISH and mounting the coverslips in DAPI containing mounting media (Vectashield, Vector Laboratories), nuclei were observed on a Nikon Eclipse E800 microscope by using a 100× Apo 1.4NA oil objective (Nikon), and using a triple filter (Nikon) to allow simultaneous visualization of FITC, TRITC, and DAPI for colocalization counts or single filters (Nikon) for copy number analysis. The percentage of cells where at least 1 pair of heterologous loci were in close spatial proximity, defined as <400 nm apart, were determined from 206 to 245 nuclei per gene pair, in each cell line analyzed. Pairwise comparisons were performed by using Yates-correlated χ^2 analysis, and $P < 0.05$ was considered significant. The identical BAC clones for *NPM1* and *ALK* as well as LSI *ALK* (Abbott Molecular) were used for conventional 2-color FISH-analysis of metaphase spreads after premature chromosome condensation. Image acquisition and analysis was performed by using an automated Olympus epifluorescence microscope (BX61) equipped with band specific optical filters (Chroma Technology Corporation) and dedicated FISH-software (Applied Spectral Imaging). For delineation of genomic changes of the *FRA2* and *ID2* gene loci, FISH analyses by using BAC clones RP11-731I19, RP11-807A19, and RP11-434B12 (German Resource Center) were performed as described (42). Tumor signals were scored as low level gains if 3–4, as amplifications if >4 copies were detectable in >10% of cells.

IR of Cells, Comet Assay, Detection of Phospho-H2AX-Foci, and Analysis of Apoptosis. Cells were irradiated with the doses indicated in the figures. Protocols were optimized for each cell line to ensure comparable induction of H2AX-phosphorylation (γ-H2AX) and percentages of viable cells after IR. DNA damage at the single cell level was analyzed 10 min after IR by using the Comet Assay (4250-050-K; Trevigen). For the detection of phospho-histone H2AX foci, cytospins of untreated cells, and cells 6 or 24 h after IR, were prepared and stained by using a FITC-conjugated phospho-Histone H2AX (ser139) antibody (16-202A; Upstate Biotechnology). In parallel, Western blot analysis for the detection of phospho-H2AX (Ser-139) was performed. Analysis of apoptosis was performed as described (6). All assays were performed in triplicate.

Immunohistology. The use of human material was approved by the ethics committee of the Charité, Medical University Berlin. Immunohistological analyses were performed as described (14) by using various antibodies (*SI Appendix*).

ACKNOWLEDGMENTS. This manuscript is dedicated to our friend and coworker Andreas Lietz, who died during the work on the project. We thank Franziska Hummel (Berlin), Simone Kressmann (Berlin), Brigitte Wollert-Wulf (Berlin), Constanze Cieluch (Berlin), Arleta Frensel (Dresden), and Petra Freitag (Dresden) for outstanding technical assistance, Peter Rahn (Berlin) for cell sorting, and Christin Wolfram (Berlin) for helpful discussion. The Fra2-JunB single-chain construct was kindly provided by Latifa Bakiri (Institut Pasteur, Paris). This work was supported in part by grants from the Deutsche Forschungsgemeinschaft, the Wilhelm Sander-Stiftung, the Berliner Krebsgesellschaft, and the Intramural Research Program of the National Institutes of Health, National Cancer Institute, Center for Cancer Research.

1. Mitelman F, Johansson B, Mertens F (2007) The impact of translocations and gene fusions on cancer causation. *Nat Rev Cancer* 7:233–245.
2. Janz S, Potter M, Rabkin CS (2003) Lymphoma- and leukemia-associated chromosomal translocations in healthy individuals. *Genes Chromosomes Cancer* 36:211–223.
3. Chiarle R, Voena C, Ambrogio C, Piva R, Inghirami G (2008) The anaplastic lymphoma kinase in the pathogenesis of cancer. *Nat Rev Cancer* 8:11–23.
4. Stein H, et al. (2000) CD30(+) anaplastic large cell lymphoma: A review of its histopathologic, genetic, and clinical features. *Blood* 96:3681–3695.
5. Mathas S, et al. (2005) Elevated NF-kappaB p50 complex formation and Bcl-3 expression in classical Hodgkin, anaplastic large-cell, and other peripheral T-cell lymphomas. *Blood* 106:4287–4293.
6. Janz M, et al. (2006) Classical Hodgkin lymphoma is characterized by high constitutive expression of activating transcription factor 3 (ATF3), which promotes viability of Hodgkin/Reed-Sternberg cells. *Blood* 107:2536–2539.
7. Willemze R, et al. (2005) WHO-EORTC classification for cutaneous lymphomas. *Blood* 105:3768–3785.
8. Meaburn KJ, Misteli T, Soutoglou E (2007) Spatial genome organization in the formation of chromosomal translocations. *Semin Cancer Biol* 17:80–90.
9. Nikiforova MN, et al. (2000) Proximity of chromosomal loci that participate in radiation-induced rearrangements in human cells. *Science* 290:138–141.
10. Aten JA, et al. (2004) Dynamics of DNA double-strand breaks revealed by clustering of damaged chromosome domains. *Science* 303:92–95.
11. Soutoglou E, et al. (2007) Positional stability of single double-strand breaks in mammalian cells. *Nat Cell Biol* 9:675–682.
12. Roix JJ, et al. (2003) Spatial proximity of translocation-prone gene loci in human lymphomas. *Nat Genet* 34:287–291.
13. Neves H, Ramos C, da Silva MG, Parreira A, Parreira L (1999) The nuclear topography of ABL, BCR, PML, and RARalpha genes: Evidence for gene proximity in specific phases of the cell cycle and stages of hematopoietic differentiation. *Blood* 93:1197–1207.
14. Mathas S, et al. (2006) Intrinsic inhibition of transcription factor E2A by HLH proteins ABF-1 and Id2 mediates reprogramming of neoplastic B cells in Hodgkin lymphoma. *Nat Immunol* 7:207–215.
15. Perk J, Iavarone A, Benezra R (2005) Id family of helix-loop-helix proteins in cancer. *Nat Rev Cancer* 5:603–614.
16. van Dam H, Castellazzi M (2001) Distinct roles of Jun : Fos and Jun : ATF dimers in oncogenesis. *Oncogene* 20:2453–2464.
17. Roussel MF, et al. (1987) Transforming potential of the c-fms proto-oncogene (CSF-1 receptor). *Nature* 325:549–552.
18. Sapi E, et al. (1999) Effect of all-trans-retinoic acid on c-fms proto-oncogene [colony-stimulating factor 1 (CSF-1) receptor] expression and CSF-1-induced invasion and anchorage-independent growth of human breast carcinoma cells. *Cancer Res* 59:5578–5585.
19. Cotta CV, et al. (2008) The helix-loop-helix protein Id2 is expressed differentially and induced by myc in T-cell lymphomas. *Cancer* 112:552–561.
20. Mathas S, et al. (2002) Aberrantly expressed c-Jun and JunB are a hallmark of Hodgkin lymphoma cells, stimulate proliferation and synergize with NF-kappa B. *EMBO J* 21:4104–4113.
21. Mao X, et al. (2003) Amplification and overexpression of JUNB is associated with primary cutaneous T-cell lymphomas. *Blood* 101:1513–1519.
22. Rothenberg EV, Moore JE, Yui MA (2008) Launching the T-cell-lineage developmental programme. *Nat Rev Immunol* 8:9–21.
23. Bonzheim I, et al. (2004) Anaplastic large cell lymphomas lack the expression of T-cell receptor molecules or molecules of proximal T-cell receptor signaling. *Blood* 104:3358–3360.
24. Osborne CS, et al. (2007) Myc dynamically and preferentially relocates to a transcription factory occupied by Igh. *PLoS Biol* 5:1763–1772.
25. Miething C, et al. (2003) The oncogenic fusion protein nucleophosmin-anaplastic lymphoma kinase (NPM-ALK) induces two distinct malignant phenotypes in a murine retroviral transplantation model. *Oncogene* 22:4642–4647.
26. Beylot-Barry M, Groppi A, Vergier B, Pulford K, Merlio JP (1998) Characterization of t(2;5) reciprocal transcripts and genomic breakpoints in CD30+ cutaneous lymphoproliferations. *Blood* 91:4668–4676.
27. Hinshaw M, et al. (2004) Three children with CD30 cutaneous anaplastic large cell lymphomas bearing the t(2;5)(p23;q35) translocation. *Pediatr Dermatol* 21:212–217.
28. Nakayama T, et al. (2007) Aberrant expression of Fra-2 promotes CCR4 expression and cell proliferation in adult T-cell leukemia. *Oncogene* 27:3221–3232.
29. Passegue E, Wagner EF, Weissman IL (2004) JunB deficiency leads to a myeloproliferative disorder arising from hematopoietic stem cells. *Cell* 119:431–443.
30. Lietz A, et al. (2007) Loss of bHLH transcription factor E2A activity in primary effusion lymphoma confers resistance to apoptosis. *Br J Haematol* 137:342–348.
31. Bain G, et al. (1997) E2A deficiency leads to abnormalities in alphabeta T-cell development and to rapid development of T-cell lymphomas. *Mol Cell Biol* 17:4782–4791.
32. Borzillo GV, Ashmun RA, Sherr CJ (1990) Macrophage lineage switching of murine early pre-B lymphoid cells expressing transduced fms genes. *Mol Cell Biol* 10:2703–2714.
33. Ait-Tahar K, et al. (2006) B and CTL responses to the ALK protein in patients with ALK-positive ALCL. *Int J Cancer* 118:688–695.
34. Halazonetis TD, Gorgoulis VG, Bartek J (2008) An oncogene-induced DNA damage model for cancer development. *Science* 319:1352–1355.
35. Mason DY, et al. (2008) in *WHO Classification of Tumours of Hematopoietic and Lymphoid Tissues*, eds Swerdlow SH, et al. (International Agency for Research on Cancer, Lyon, France), pp 317–319.
36. Pombo A, Branco MR (2007) Functional organisation of the genome during interphase. *Curr Opin Genet Dev* 17:451–455.
37. Osborne CS, et al. (2004) Active genes dynamically colocalize to shared sites of ongoing transcription. *Nat Genet* 36:1065–1071.
38. Pratt-Hyatt MJ, Kapadia KM, Wilson TE, Engelke DR (2006) Increased recombination between active tRNA genes. *DNA Cell Biol* 25:359–364.
39. Behre G, et al. (1999) c-Jun is a JNK-independent coactivator of the PU. 1 transcription factor. *J Biol Chem* 274:4939–4946.
40. Bakiri L, Matsuo K, Wisniewska M, Wagner EF, Yaniv M (2002) Promoter specificity and biological activity of tethered AP-1 dimers. *Mol Cell Biol* 22:4952–4964.
41. Meaburn KJ, Misteli T (2008) Locus-specific and activity-independent gene repositioning during early tumorigenesis. *J Cell Biol* 180:39–50.
42. Freier K, et al. (2003) Tissue microarray analysis reveals site-specific prevalence of oncogene amplifications in head and neck squamous cell carcinoma. *Cancer Res* 63:1179–1182.